

# Nonlinear Power Amplifier-Resilient Cell-Free Massive MIMO: A Joint Optimization Approach

Wei Jiang, *Senior Member, IEEE*, and Hans Dieter Schotten, *Member, IEEE*

**Abstract**—This letter analyzes the effects of power amplifiers (PAs) on the downlink of cell-free massive MIMO systems. We model signal transmission incorporating nonlinear PA distortion and derive a unified spectral efficiency (SE) expression applicable to arbitrary precoding schemes. To combat PA-induced performance degradation, a joint optimization approach for user association and max-min power control is proposed. Furthermore, a low-complexity alternative is developed to approximate the joint optimization with reduced computational overhead. Simulations validate the analysis and demonstrate significant performance gains of the proposed approaches over conventional techniques.

**Index Terms**—Cell-free massive MIMO, max-min power control, nonlinear power amplifier, user association, user fairness

## I. INTRODUCTION

CELL-FREE (CF) massive multi-input multi-output (CF-mMIMO) has garnered significant attention for its ability to provide uniformly high-quality service across the entire coverage area, effectively eliminating the cell-edge under-service problem that has plagued conventional cellular systems for decades [1]. Nevertheless, power amplifiers (PAs)—critical components in wireless transmitters—introduce nonlinear signal distortion, particularly when operating near their saturation point. This nonlinearity distorts the transmitted signal, affecting the desired signal strength and introducing additional interference. Ignoring it can lead to overestimated system performance and cause bias into algorithm design.

To date, the existing CF-mMIMO studies totally neglected this major hardware impairment, with only a few works providing initial insights. Mokhtari et al. [2] quantified sum-rate degradation under PA distortion using maximum ratio (MR) precoding with equal power allocation. Subsequent studies by Jadidi et al. [3] and Khoueini et al. [4] investigated uplink and downlink impacts, respectively, assuming single-antenna access points (APs) and MR precoding. While these studies offer valuable theoretical insights, several key dimensions remain unexplored, e.g.,

- *Scalability limits*: [2]–[4] use conventional CF configuration where all APs serve all users, neglecting the scalability gain of user-centric dynamic clustering [5];
- *Precoding generality constraint*: [2]–[4] focus solely on MR precoding, omitting state-of-the-art techniques such as zero-forcing (ZF) [6] and minimum mean square error (MMSE) precoding [7], which can more effectively mitigate multi-user interference.

To bridge these gaps, this letter presents a unified analytical framework and a novel design for PA-resilient CF-mMIMO systems. Specifically, we develop a downlink signal model that captures nonlinear PA distortion at spatially correlated multi-antenna APs, and derive a spectral efficiency (SE) expression applicable to arbitrary linear precoding schemes—including MR, ZF, regularized ZF (RZF), and MMSE precoding. Our analysis reveals that the achievable SE under PA-induced distortion critically depends on both user association and power control. Leveraging this insight, we propose a joint optimization approach that adaptively handles user-centric AP association and max-min fairness power allocation to effectively suppress nonlinear distortion. Furthermore, a low-complexity alternative is developed to approximate the joint solution with reduced computational overhead. Numerical evaluation in terms of SE performance and computational complexity is performed.

The remainder of this letter is structured as follows. Section II introduces the system model. Section III presents the SE analysis under PA distortion. Section IV formulates the joint optimization design. Section V analyzes computational complexity and offers a low-complexity algorithm. Finally, Section VI validates the gains via simulations.

## II. SYSTEM MODEL

We consider a CF-mMIMO system comprising  $L$  APs, each equipped with  $N_a$  co-located antennas, distributed throughout a coverage area to serve  $K$  users. To exploit channel hardening, the total number of antennas  $M = L \times N_a$  should be large, satisfying  $M \gg K$ . Each user equipment (UE) is generally equipped with a single antenna. The sets of indices for APs and users are denoted by  $\mathbb{L} = \{1, \dots, L\}$  and  $\mathbb{K} = \{1, \dots, K\}$ , respectively. The wireless channel from AP  $l$ ,  $\forall l \in \mathbb{L}$  to UE  $k$ ,  $\forall k \in \mathbb{K}$  is denoted by  $\mathbf{h}_{kl} \in \mathbb{C}^{N_a}$ . Adopting the block fading assumption, each *coherent block*—a time-frequency span of  $\tau_c$  symbols—maintains a quasi-static channel response. In practical deployments, closely spaced antennas at an AP exhibit spatial correlation due to their physical proximity. Hence, each coherence block applies an independent realization from *correlated* Rayleigh fading, defined as  $\mathbf{h}_{kl} \sim \mathcal{CN}(\mathbf{0}, \mathbf{R}_{kl})$ , where  $\mathbf{R}_{kl} = \mathbb{E}[\mathbf{h}_{kl}\mathbf{h}_{kl}^H]$  stands for the spatial correlation matrix. Using linear MMSE estimation [7], the estimated channel  $\hat{\mathbf{h}}_{kl}$  follows a complex Gaussian distribution  $\hat{\mathbf{h}}_{kl} \sim \mathcal{CN}(\mathbf{0}, p_u \tau_p \mathbf{R}_{kl} \mathbf{\Gamma}_{kl}^{-1} \mathbf{R}_{kl})$ , where  $\mathbf{\Gamma}_{kl} = p_u \tau_p \sum_{k' \in \mathcal{P}_k} \mathbf{R}_{kl'} + \sigma_z^2 \mathbf{I}_{N_a}$ , and  $p_u$  denotes the maximal transmit power of the UEs,  $\tau_p$  is the pilot sequence length,  $\mathcal{P}_k$  is the set of users sharing the same pilot as user  $k$ , and  $\sigma_z^2$  indicates the variance of thermal noise. The

W. Jiang and H. D. Schotten are with German Research Center for Artificial Intelligence (DFKI), Kaiserslautern, Germany, and are also with the University of Kaiserslautern (RPTU), Germany.

estimation error, defined as  $\tilde{\mathbf{h}}_{kl} = \mathbf{h}_{kl} - \hat{\mathbf{h}}_{kl}$ , is attributed to both noise and pilot contamination, following  $\mathcal{CN}(\mathbf{0}, \mathbf{\Theta}_{kl})$ , where the associated error covariance matrix is given by  $\mathbf{\Theta}_{kl} = \mathbb{E}[\tilde{\mathbf{h}}_{kl}\tilde{\mathbf{h}}_{kl}^H] = \mathbf{R}_{kl} - p_u\tau_p\mathbf{R}_{kl}\mathbf{\Gamma}_{kl}^{-1}\mathbf{R}_{kl}$ .

### III. DOWNLINK TRANSMISSION

In the downlink, the data symbols intended for the  $K$  users are assumed to be independent, zero-mean random variables with unit variance. These symbols are jointly expressed as  $\mathbf{x} = [x_1, \dots, x_K]^T$ , satisfying  $\mathbb{E}[\mathbf{x}\mathbf{x}^H] = \mathbf{I}_K$ . Under the user-centric dynamic clustering strategy, each AP maintains a set of associated users, denoted by  $\mathbb{K}_l$  for AP  $l$ , where the set can vary from empty, i.e.,  $\mathbb{K}_l = \emptyset$ , to the complete user set  $\mathbb{K}_l = \mathbb{K}$ . Each AP spatially multiplexes the symbols of its associated users  $k \in \mathbb{K}_l$ , producing

$$\mathbf{s}_l = \sqrt{p_a} \sum_{k \in \mathbb{K}_l} u_{kl} \sqrt{\eta_{kl}} \mathbf{w}_{kl} x_k, \quad (1)$$

where  $p_a$  denotes the AP power constraint,  $\eta_{kl}$  is the power coefficient for AP  $l$  to user  $k$ ,  $u_{kl}$  is the AP-UE-association indicator, which equals 1 if user  $k$  is served by AP  $l$  (i.e.,  $k \in \mathbb{K}_l$ ), and 0 otherwise. The vector  $\mathbf{w}_{kl} \in \mathbb{C}^{N_a}$  denotes the precoding vector employed by AP  $l$  for user  $k$ , with the normalization constraint  $\mathbb{E}[\|\mathbf{w}_{kl}\|^2] = 1$ .

#### A. Nonlinear Power Amplification

A common approach to model PA nonlinearity is the Bussgang decomposition, which represents the PA output for a zero-mean Gaussian input signal as a linear component plus an uncorrelated distortion term. For the feeding signal  $\mathbf{s}_l$ , the amplified transmit signal at AP  $l$  is given by

$$\mathbf{x}_l = \mathcal{G}(\mathbf{s}_l) = \alpha_l \sqrt{p_a} \sum_{k \in \mathbb{K}_l} u_{kl} \sqrt{\eta_{kl}} \mathbf{w}_{kl} x_k + \mathbf{d}_l, \quad (2)$$

where:

- $\mathcal{G}(\cdot)$ : Nonlinear PA function, e.g., the Rapp model, described by  $\mathcal{G}(s) = s / (1 + (|s|/A_s)^{2\xi})^{1/2\xi}$ , where  $s$  is the input,  $A_s$  denotes the saturation level, and  $\xi$  controls the smoothness of the transition to saturation.
- $\alpha_l$  is a complex linear gain, and  $\alpha_l = \mathbb{E}[\mathbf{s}_l^H \mathcal{G}(\mathbf{s}_l)] / \mathbb{E}[\|\mathbf{s}_l\|^2]$ .
- $\mathbf{d}_l \sim \mathcal{CN}(0, \sigma_d^2 \mathbf{I}_{N_a})$  is complex Gaussian distortion, uncorrelated with  $\mathbf{s}_l$  (i.e.,  $\mathbb{E}[\mathbf{s}_l^H \mathbf{d}_l] = \mathbf{0}$ ), where

$$\sigma_d^2 = \beta_l \mathbb{E}[\|\mathbf{s}_l\|^2] = \beta_l p_a \sum_{k \in \mathbb{K}_l} u_{kl} \eta_{kl} \quad (3)$$

stands for distortion variance, and  $\beta_l$  represents distortion-to-signal ratio.

Thus, the actual transmitted power is expressed by

$$\begin{aligned} \mathbb{E}[\|\mathbf{x}_l\|^2] &= \mathbb{E}\left[\left\|\alpha_l \sqrt{p_a} \sum_{k \in \mathbb{K}_l} u_{kl} \sqrt{\eta_{kl}} \mathbf{w}_{kl} x_k + \mathbf{d}_l\right\|^2\right] \\ &= |\alpha_l|^2 p_a \sum_{k \in \mathbb{K}_l} u_{kl} \eta_{kl} \mathbb{E}[\|\mathbf{w}_{kl}\|^2] + \mathbb{E}[\|\mathbf{d}_l\|^2], \end{aligned} \quad (4)$$

applying  $u_{kl}^2 = u_{kl}$ . The distortion power is

$$\mathbb{E}[\|\mathbf{d}_l\|^2] = \text{tr}(\mathbb{E}[\mathbf{d}_l \mathbf{d}_l^H]) = \text{tr}(\sigma_d^2 \mathbf{I}_{N_a}) = \beta_l p_a N_a \sum_{k \in \mathbb{K}_l} u_{kl} \eta_{kl},$$

since  $\mathbb{E}[\|\mathbf{w}_{kl}\|^2] = 1$ . Now, (4) simplifies to  $\mathbb{E}[\|\mathbf{x}_l\|^2] = (|\alpha_l|^2 p_a + \beta_l p_a N_a) \sum_{k \in \mathbb{K}_l} u_{kl} \eta_{kl}$ . To ensure the AP respects its power budget, the transmitted power must satisfy  $\mathbb{E}[\|\mathbf{x}_l\|^2] \leq p_a$ , imposing the constraint:

$$\sum_{k \in \mathbb{K}_l} u_{kl} \eta_{kl} \leq \frac{1}{|\alpha_l|^2 + \beta_l N_a}, \quad \forall l \in \mathbb{L}. \quad (5)$$

#### B. Precoding Schemes

To ensure scalability, each AP  $l$  independently performs local signal processing using its own channel estimates, denoted by  $\hat{\mathbf{H}}_l = [\hat{\mathbf{h}}_{l1}, \dots, \hat{\mathbf{h}}_{lK}] \in \mathbb{C}^{N_a \times K}$ . The applicable precoding schemes identified include:

- 1) **MR**: This simple approach, a.k.a. conjugate beamforming, sets the precoding matrix at AP  $l$  as  $\mathbf{V}_l^{mr} = \hat{\mathbf{H}}_l^*$  to maximize the desired signal strength.
- 2) **ZF**: Aiming to cancel multi-user interference, the ZF precoder is the pseudo-inverse of  $\hat{\mathbf{H}}_l$ , given by  $\mathbf{V}_l^{zf} = \hat{\mathbf{H}}_l^* (\hat{\mathbf{H}}_l^T \hat{\mathbf{H}}_l^*)^{-1}$  so as to meet  $\hat{\mathbf{H}}_l^T \mathbf{V}_l^{zf} = \mathbf{I}_K$ . This condition holds exclusively when the channel matrix satisfies the full-rank assumption, when  $\hat{\mathbf{H}}_l$  has full column rank, requiring  $N_a \geq K$ .
- 3) **RZF**: In practice, due to scalability requirement, APs may be equipped with fewer antennas than users ( $N_a < K$ ), rendering ZF inapplicable. To handle rank-deficient cases, regularized ZF is used, i.e.,  $\mathbf{V}_l^{rzf} = \hat{\mathbf{H}}_l^* (\hat{\mathbf{H}}_l^T \hat{\mathbf{H}}_l^* + \sigma_z^2 \mathbf{I}_K)^{-1}$ , where the regularization term  $\sigma_z^2 \mathbf{I}_K$  ensures matrix invertibility.
- 4) **MMSE**: The balance between interference suppression and noise enhancement is achieved by minimizing the mean squared error (MSE) between the transmitted symbols and the received signal. The MMSE precoding matrix is given by

$$\mathbf{V}_l^{\text{mmse}} = (p_u \hat{\mathbf{H}}_l \mathbf{E}_l \hat{\mathbf{H}}_l^H + p_u \sum_{k \in \mathbb{K}} \eta_{kl} \mathbf{\Theta}_{kl} + \sigma_z^2 \mathbf{I}_{N_a})^{-1} \hat{\mathbf{H}}_l, \quad (6)$$

where  $\mathbf{E}_l = \text{diag}(\eta_{l1}, \dots, \eta_{lK})$  is a diagonal matrix of power coefficients.

Let  $\mathbf{v}_{kl} \in \mathbb{C}^{N_a}$  denote the  $k$ -th column of  $\mathbf{V}_l \in \mathbb{C}^{N_a \times K}$ , i.e.,  $\mathbf{v}_{kl} = \mathbf{V}_l(:, k)$ . The required precoding vector  $\mathbf{w}_{kl}$  is obtained by normalizing  $\mathbf{v}_{kl}$  as

$$\mathbf{w}_{kl} = \frac{\mathbf{v}_{kl}}{\|\mathbf{v}_{kl}\|}, \quad \forall l \in \mathbb{L}, \forall k \in \mathbb{K}, \quad (7)$$

ensuring it satisfies the normalization condition  $\mathbb{E}[\|\mathbf{w}_{kl}\|^2] = 1$ .

#### C. Performance Analysis

The received signal at user  $k$  is  $y_k = \sum_{l \in \mathbb{L}} \mathbf{h}_{kl}^T \mathbf{x}_l + n_k$ , where noise  $n_k \sim \mathcal{CN}(0, \sigma_z^2)$ . The expression can be expanded as

$$y_k = \sqrt{p_a} \sum_{l \in \mathbb{L}} \alpha_l \sum_{k' \in \mathbb{K}} u_{k'l} \sqrt{\eta_{k'l}} \mathbf{h}_{kl}^T \mathbf{w}_{k'l} x_{k'} + \sum_{l \in \mathbb{L}} \mathbf{h}_{kl}^T \mathbf{d}_l + n_k. \quad (8)$$

In massive MIMO systems, users typically does not know channel estimates due to the absence of downlink pilots, making coherent detection impractical. Instead, signal detection is performed using large-scale fading decoding (LSFD), where the statistical mean  $\mathbb{E}[\mathbf{w}_{kl}^H \hat{\mathbf{h}}_{kl}]$ ,  $\forall k, l$ , serves as an approximation. This statistical mismatch leads to an additional

performance degradation known as channel uncertainty error. To facilitate the derivation, (8) is decomposed into

$$\begin{aligned}
 y_k = & \underbrace{\sqrt{p_a} \sum_{l \in \mathbb{L}} \alpha_l u_{kl} \sqrt{\eta_{kl}} \mathbb{E}[\mathbf{h}_{kl}^T \mathbf{w}_{kl}]}_{\mathcal{S}_1: \text{desired signal over channel statistics}} x_k \\
 & + \underbrace{\sqrt{p_a} \sum_{l \in \mathbb{L}} \alpha_l u_{kl} \sqrt{\eta_{kl}} (\mathbf{h}_{kl}^T \mathbf{w}_{kl} - \mathbb{E}[\mathbf{h}_{kl}^T \mathbf{w}_{kl}])}_{\mathcal{J}_1: \text{channel uncertainty error}} x_k \\
 & + \underbrace{\sqrt{p_a} \sum_{l \in \mathbb{L}} \alpha_l \sum_{k' \in \mathbb{K} \setminus \{k\}} u_{k'l} \sqrt{\eta_{k'l}} \mathbf{h}_{kl}^T \mathbf{w}_{k'l}}_{\mathcal{J}_2: \text{inter-user interference}} x_{k'} + \underbrace{\sum_{l \in \mathbb{L}} \mathbf{h}_{kl}^T \mathbf{d}_l}_{\mathcal{J}_3: \text{PA distortion}} + n_k.
 \end{aligned} \quad (9)$$

**Proposition 1:** The achievable SE of user  $k$  is  $R_k = \mathbb{E}[\log_2(1 + \gamma_k)]$ , where the instantaneous effective SINR is

$$\gamma_k = \frac{|\sum_{l \in \mathbb{L}} \alpha_l u_{kl} \sqrt{\eta_{kl}} \mathbb{E}[\mathbf{h}_{kl}^T \mathbf{w}_{kl}]|^2}{\left\{ \sigma_z^2 / p_a + \sum_{k' \in \mathbb{K}} \left( \sum_{l \in \mathbb{L}} u_{k'l} \eta_{k'l} |\alpha_l|^2 \mathbb{E}[\|\mathbf{h}_{k'l}^T \mathbf{w}_{k'l}\|^2] \right) - \sum_{l \in \mathbb{L}} u_{kl} \eta_{kl} |\alpha_l|^2 |\mathbb{E}[\mathbf{h}_{kl}^T \mathbf{w}_{kl}]|^2 + \sum_{l \in \mathbb{L}} \beta_l \left( \sum_{k' \in \mathbb{K}} u_{k'l} \eta_{k'l} \right) \text{tr}(\mathbf{R}_{kl}) \right\}} \quad (10)$$

*Proof:* The SINR is computed by  $\gamma_k = \frac{|\mathcal{S}_1|^2}{\mathbb{E}[\mathcal{J}_1 + \mathcal{J}_2 + \mathcal{J}_3] + \sigma_z^2}$ , where the power gain of the desired signal is

$$|\mathcal{S}_1|^2 = p_a \left| \sum_{l \in \mathbb{L}} \alpha_l u_{kl} \sqrt{\eta_{kl}} \mathbb{E}[\mathbf{h}_{kl}^T \mathbf{w}_{kl}] \right|^2. \quad (11)$$

Due to the independence among data symbols and signal distortion,  $\mathcal{J}_1$ ,  $\mathcal{J}_2$ , and  $\mathcal{J}_3$  in (9) are uncorrelated. This implies that  $\mathbb{E}[\mathcal{J}_1 + \mathcal{J}_2 + \mathcal{J}_3] = \mathbb{E}[\mathcal{J}_1] + \mathbb{E}[\mathcal{J}_2] + \mathbb{E}[\mathcal{J}_3]$ . We now compute the variance of  $\mathcal{J}_1$  as

$$\begin{aligned}
 \mathbb{E}[\mathcal{J}_1^2] &= p_a \sum_{l \in \mathbb{L}} u_{kl} \eta_{kl} |\alpha_l|^2 \mathbb{E}[\|\mathbf{h}_{kl}^T \mathbf{w}_{kl} - \mathbb{E}[\mathbf{h}_{kl}^T \mathbf{w}_{kl}]\|^2] \\
 &= p_a \sum_{l \in \mathbb{L}} u_{kl} \eta_{kl} |\alpha_l|^2 \left( \mathbb{E}[\|\mathbf{h}_{kl}^T \mathbf{w}_{kl}\|^2] - |\mathbb{E}[\mathbf{h}_{kl}^T \mathbf{w}_{kl}]|^2 \right).
 \end{aligned} \quad (12)$$

Next, the variance of  $\mathcal{J}_2$  is computed as

$$\mathbb{E}[\mathcal{J}_2^2] = p_a \sum_{l \in \mathbb{L}} |\alpha_l|^2 \sum_{k' \in \mathbb{K} \setminus \{k\}} u_{k'l} \eta_{k'l} \mathbb{E}[\|\mathbf{h}_{k'l}^T \mathbf{w}_{k'l}\|^2].$$

Finally,

$$\mathbb{E}[\mathcal{J}_3^2] = \sum_{l \in \mathbb{L}} \sigma_d^2 \mathbb{E}[\|\mathbf{h}_{kl}\|^2] = p_a \sum_{l \in \mathbb{L}} \beta_l \left( \sum_{k' \in \mathbb{K}} u_{k'l} \eta_{k'l} \right) \text{tr}(\mathbf{R}_{kl}).$$

Applying  $\mathcal{S}_1$ ,  $\mathcal{J}_1$ ,  $\mathcal{J}_2$ , and  $\mathcal{J}_3$  yields (10). ■

#### IV. JOINT OPTIMIZATION OF USER ASSOCIATION AND MAX-MIN POWER ALLOCATION

Analyzing (10) reveals that the achievable SINR depends on two adaptive mechanisms: user-centric AP association ( $u_{kl}$ ) and power control ( $\eta_{kl}$ ). To perserve uniformly high-quality service under PA-induced distortion, we propose jointly optimizing user association and max-min power allocation. The problem formulation is

$$\begin{aligned}
 \max_{\mathbf{U}, \boldsymbol{\eta}} \quad & \min_{k \in \mathbb{K}} \gamma_k \\
 \text{s.t.} \quad & \begin{cases} \sum_{k \in \mathbb{K}} u_{kl} \eta_{kl} \leq \frac{1}{|\alpha_l|^2 + \beta_l N_a}, \quad \forall l \in \mathbb{L}, \\ \eta_{kl} \geq 0, \quad u_{kl} \in \{0, 1\}, \quad \forall k \in \mathbb{K}, l \in \mathbb{L}, \end{cases}
 \end{aligned} \quad (13)$$

where  $\mathbf{U} = [u_{kl}]$  is the binary association matrix, and  $\boldsymbol{\eta} = [\eta_{kl}]$  is the power allocation matrix. The numerator of  $\gamma_k$  is a square of a sum of square roots, which is not convex in  $\boldsymbol{\eta}$ . To convexify this term, we introduce auxiliary variables  $v_{kl}$ , collectively denoted as  $\mathbf{v} = \{v_{kl}\}_{k \in \mathbb{K}, l \in \mathbb{L}}$ , and impose the following constraint:

$$v_{kl}^2 \leq \eta_{kl}, \quad \forall k \in \mathbb{K}, l \in \mathbb{L}. \quad (14)$$

This can be rewritten as a convex rotated second-order cone (SOC) constraint, i.e.,

$$\|[2v_{kl}; 1 - \eta_{kl}]\| \leq 1 + \eta_{kl}, \quad \forall k \in \mathbb{K}, l \in \mathbb{L}. \quad (15)$$

With this substitution, the effective received signal for user  $k$  can be denoted by

$$\mathcal{A}_k(\mathbf{U}, \mathbf{v}) = \sum_{l \in \mathbb{L}} \alpha_l u_{kl} v_{kl} \mathbb{E}[\mathbf{h}_{kl}^T \mathbf{w}_{kl}],$$

which becomes linear in  $v_{kl}$ .

Define the additive terms in the denominator of (10) as

$$\begin{aligned}
 \mathcal{B}_k(\mathbf{U}, \mathbf{v}) &= \sum_{k' \in \mathbb{K}} \left( \sum_{l \in \mathbb{L}} u_{k'l} v_{k'l}^2 |\alpha_l|^2 \mathbb{E}[\|\mathbf{h}_{k'l}^T \mathbf{w}_{k'l}\|^2] \right) \\
 &+ \sum_{l \in \mathbb{L}} \beta_l \left( \sum_{k' \in \mathbb{K}} u_{k'l} v_{k'l}^2 \right) \text{tr}(\mathbf{R}_{kl}) + \sigma_z^2 / p_a,
 \end{aligned} \quad (16)$$

and the subtracted term as  $C_k(\mathbf{U}, \mathbf{v}) = \sum_{l \in \mathbb{L}} u_{kl} v_{kl}^2 |\alpha_l|^2 |\mathbb{E}[\mathbf{h}_{kl}^T \mathbf{w}_{kl}]|^2$ . Thus, the denominator becomes  $\mathcal{B}_k(\mathbf{U}, \mathbf{v}) - C_k(\mathbf{U}, \mathbf{v})$ . Introducing a slack variable  $\gamma_t$  to represent the common SINR target, the constraint  $\gamma_k \geq \gamma_t$  is rewritten to

$$|\mathcal{A}_k(\mathbf{U}, \mathbf{v})|^2 \geq \gamma_t (\mathcal{B}_k(\mathbf{U}, \mathbf{v}) - C_k(\mathbf{U}, \mathbf{v})), \quad \forall k \in \mathbb{K}, \quad (17)$$

which is still non-convex due to the quadratic term  $|\mathcal{A}_k(\mathbf{U}, \mathbf{v})|^2$  on the left-hand side. To convexify (17), we make use of the fact that  $|\mathcal{A}_k(\mathbf{U}, \mathbf{v})| \geq \Re\{\mathcal{A}_k(\mathbf{U}, \mathbf{v})\}$  and  $C_k(\mathbf{U}, \mathbf{v}) \geq 0$ , leading to a stricter constraint:

$$(\Re\{\mathcal{A}_k(\mathbf{U}, \mathbf{v})\})^2 \geq \gamma_t \mathcal{B}_k(\mathbf{U}, \mathbf{v}), \quad \forall k \in \mathbb{K}. \quad (18)$$

This implies that any solution satisfying (18) automatically satisfies the original constraint (17). Since  $\Re\{\mathcal{A}_k(\mathbf{U}, \mathbf{v})\}$  is linear in  $v_{kl}$ , we reformulate (18) into an SOC form:

$$\Re\{\mathcal{A}_k(\mathbf{U}, \mathbf{v})\} \geq \sqrt{\gamma_t} \|\mathbf{b}_k(\mathbf{U}, \mathbf{v})\|, \quad \forall k \in \mathbb{K}, \quad (19)$$

where  $\mathbf{b}_k(\mathbf{U}, \mathbf{v})$  is a vector that stacks the square roots of all  $\mathcal{B}_k(\mathbf{U}, \mathbf{v})$ 's terms, namely

$$\begin{aligned}
 \mathbf{b}_k(\mathbf{U}, \mathbf{v}) &= \\
 & \left[ \frac{\sigma_z}{\sqrt{p_a}}; \left\{ v_{k'l} |\alpha_l| \sqrt{u_{k'l} \mathbb{E}[\|\mathbf{h}_{k'l}^T \mathbf{w}_{k'l}\|^2]}; v_{k'l} \sqrt{u_{k'l} \beta_l \text{tr}(\mathbf{R}_{kl})} \right\}_{k' \in \mathbb{K}, l \in \mathbb{L}} \right].
 \end{aligned} \quad (20)$$

Putting all these elements together, (13) is transformed to a tractable optimization problem:

$$\begin{aligned}
 \max_{\mathbf{U}, \mathbf{v}, \gamma_t} \quad & \gamma_t \\
 \text{s.t.} \quad & \begin{cases} \Re\{\mathcal{A}_k(\mathbf{U}, \mathbf{v})\} \geq \sqrt{\gamma_t} \|\mathbf{b}_k(\mathbf{U}, \mathbf{v})\|, \quad \forall k \in \mathbb{K}, \\ \|[2v_{kl}; 1 - \eta_{kl}]\| \leq 1 + \eta_{kl}, \quad \forall k \in \mathbb{K}, l \in \mathbb{L}, \\ \sum_{k \in \mathbb{K}} u_{kl} v_{kl}^2 \leq \frac{1}{|\alpha_l|^2 + \beta_l N_a}, \quad \forall l \in \mathbb{L}, \\ v_{kl} \geq 0, \quad u_{kl} \in \{0, 1\}, \quad \forall k \in \mathbb{K}, l \in \mathbb{L}. \end{cases}
 \end{aligned} \quad (21)$$

This problem can be solved by a bisection method on  $\gamma_t$ , as depicted in Algorithm 1.

---

**Algorithm 1: Joint Optimization Approach**


---

Initialization:

$$t \leftarrow 0, \quad \gamma_{\text{low}}^{(0)} \leftarrow 0, \quad \gamma_{\text{high}}^{(0)} \leftarrow \max_{k \in \mathbb{K}} \left( \frac{p_a |\sum_{l \in \mathbb{L}} \alpha_l \mathbb{E}[\mathbf{h}_{kl}^T \mathbf{w}_{kl}]|^2}{\sigma_z^2} \right)$$

**while**  $\gamma_{\text{high}}^{(t)} - \gamma_{\text{low}}^{(t)} > \epsilon$  **do**

$$\gamma_t \leftarrow \frac{1}{2}(\gamma_{\text{low}}^{(t)} + \gamma_{\text{high}}^{(t)})$$

Convex Feasibility Check:

Find  $\{\mathbf{U}, \mathbf{v}\}$

$$\text{s.t.} \quad \begin{cases} \Re\{\mathcal{A}_k(\mathbf{U}, \mathbf{v})\} \geq \sqrt{\gamma_t} \|\mathbf{b}_k(\mathbf{U}, \mathbf{v})\|, & \forall k \in \mathbb{K}, \\ \|[2v_{kl}; 1 - \eta_{kl}]\| \leq 1 + \eta_{kl}, & \forall k \in \mathbb{K}, l \in \mathbb{L}, \\ \sum_{k \in \mathbb{K}} u_{kl} v_{kl}^2 \leq \frac{1}{|\alpha_l|^2 + \beta_l N_a}, & \forall l \in \mathbb{L}, \\ v_{kl} \geq 0, \quad u_{kl} \in \{0, 1\}, & \forall k \in \mathbb{K}, l \in \mathbb{L}. \end{cases}$$

**if feasible then**

$$\gamma_{\text{low}}^{(t+1)} \leftarrow \gamma_t, \quad \gamma_{\text{high}}^{(t+1)} \leftarrow \gamma_{\text{high}}^{(t)}, \quad \mathbf{U}^* \leftarrow \mathbf{U}, \mathbf{v}^* \leftarrow \mathbf{v}$$

**end**

**else**

$$\gamma_{\text{low}}^{(t+1)} \leftarrow \gamma_{\text{low}}^{(t)}, \quad \gamma_{\text{high}}^{(t+1)} \leftarrow \gamma_t$$

**end**

$$t \leftarrow t + 1$$

**end**

**return**  $\{\mathbf{U}^*, \mathbf{v}^*\}$

---

## V. COMPUTATIONAL COST AND LOW-COMPLEXITY ALTERNATIVE

The joint user association and power optimization (JUP) constitutes a mixed-integer SOC program. It involves  $n = L \times K$  binary variables  $u_{kl}$ , indicating user-AP associations, and up to  $n$  continuous power variables  $\eta_{kl}$ , conditioned on the associated  $u_{kl} = 1$ . In the worst case, all  $2^n$  combinations of  $\mathbf{U}$  must be explored, resulting in an exponential complexity of  $O(2^n)$ . Such exponential scaling may limit the applicability of this approach to large-scale networks. To address this challenge, we propose a two-stage decoupled strategy:

- 1) *Fixed User Association*: Each user is associated with its geographically closest AP(s), thereby eliminating the binary variables  $u_{kl}$  from the optimization problem.
- 2) *Max-Min Power Control*: With  $\mathbf{U}$  fixed, the problem reduces to optimizing  $\{\eta_{kl}\}$  to maximize the minimum achievable SE. Power is allocated only to active associations (i.e., where  $u_{kl} = 1$ ), so the effective number of power variables is smaller than  $L \times K$ .

For reference and upper-bound analysis, we compare against the conventional max-min power control [8], which optimizes all  $L \times K$  power variables. This problem is a standard SOC program with polynomial-time solvability using interior-point methods, corresponding to the complexity on the order of  $O(n^3)$ . By decoupling user association and power control, this low-complexity alternative (named JUP-Lo) enables efficient optimization for larger network deployments.

## VI. SIMULATION RESULTS AND DISCUSSIONS

This section presents numerical evaluation of the proposed joint approach in terms of spectral efficiency and compu-

TABLE I  
COMPLEXITY COMPARISON OF DIFFERENT OPTIMIZATION SCHEMES

Algorithm	JUP	JUP-Lo	Max-Min Optimization
Complexity	$O(2^{L \times K})$	$O((L \times K)^3)$	$O((L \times K)^3)$

TABLE II  
KEY SIMULATION PARAMETERS

Parameter	Value
Coverage Radius	1000 m (3GPP Microcell)
Path Loss Model	$-30.5 - 36.7 \log_{10}(d)$ (dB)
Shadow Fading	$\mathcal{N}(0, 4^2)$ dB, Gaussian normal
Number of Active Users	$K = 4$
AP Configuration	32 APs, each with 2 antennas
UE Power Constraint	$p_u = 200$ mW
AP Power Constraint	$p_a = 100$ mW
Noise Spectral Density	$-174$ dBm/Hz
Noise Figure	9 dB
System Bandwidth	5 MHz
Antenna Array Type	ULA with half-wavelength spacing
Spatial Correlation Model	Gaussian scattering [9, Sec. 2.6]
Angular Spread (Std. Dev.)	$30^\circ$
Coherence Interval	$\tau_c = 200$ channel uses
Pilot Contamination	$\tau_p = 2$ (2 users per pilot)
PA Gain Coefficients	$0.8 + 0.1i \cdot \mathcal{N}(0, 1)$ , standard normal
PA Nonlinearity Factors	$0.05 + 0.1 \cdot \mathcal{U}(0, 1)$ , uniform distribution

tational complexity. We compare its performance with four benchmark schemes: 1) CF configuration with equal power allocation (EPA); 2) CF with max-min power optimization — all APs serve all users with optimized power coefficients to maximize the worst-case SE; 3) User-centric (UC) method where each AP serves its nearest user; and 4) Ideal case without PA nonlinearity (i.e.,  $\alpha_l = 1$  and  $\beta_l = 0$ ). Key simulation parameters are listed in Table II. The performance under different precoding strategies—MR, RZF, and MMSE—is illustrated in Figs. 1a, 1b, and 1c, respectively. Each figure shows the cumulative distribution function (CDF) of SE across users. Particular attention is given to the 95%-likely SE (i.e., the 5<sup>th</sup> percentile of each CDF), which serves as a key indicator of user fairness and cell-edge performance. The mixed-integer SOC problem in (21) is implemented using CVX [10] in conjunction with the Gurobi optimizer [11].

Key observations from the numerical results are as follows:

- *PA Nonlinearity Impact*: The results show that the 95%-likely SE under nonlinear PA is very poor, i.e., 0.0024, 0.0025, and 0.0020 bps/Hz for MR, RZF, and MMSE, respectively. In contrast, in the ideal case, the SEs reach 0.5635, 0.6542, and 0.6767 bps/Hz, respectively. This wide performance gap and near-zero SE values underscore the significant adverse impact of PA nonlinearity and highlight the need for PA-resilient design.
- *Baseline Limitations*: The applied UC approach yields inferior 95%-likely SE (MR: 0.0004, RZF: 0.0003, MMSE: 0.0003 bps/Hz), evident in the CDFs' early plateaus. While reducing fronthaul overhead, its exclusion of non-nearest users creates fairness gaps. The conventional max-min power optimization performs better, achieving 0.0289, 0.0956, and 0.0268 bps/Hz under MR, RZF, and

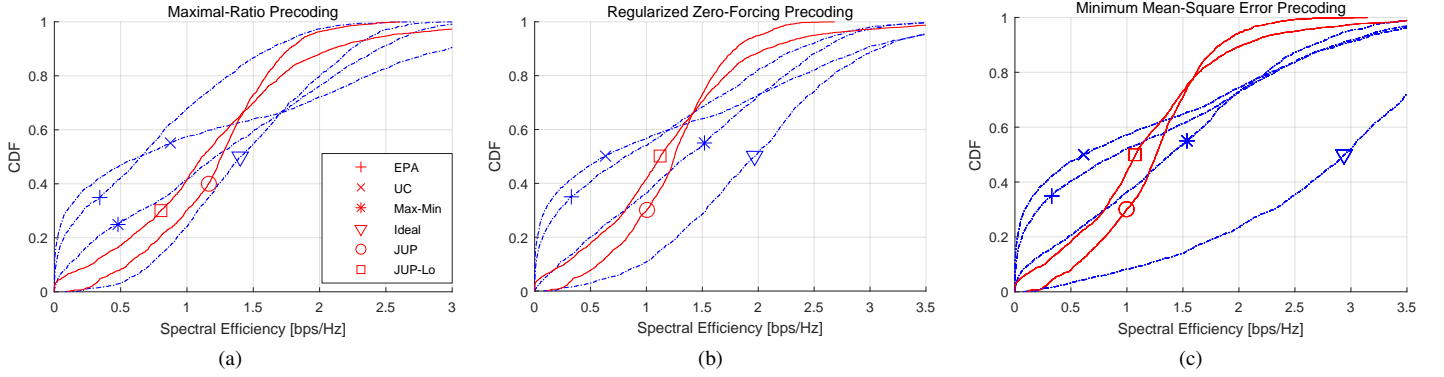


Fig. 1. The CDF of achievable spectral efficiency under MR, RZF, and MMSE precoding. User fairness (worst-case performance) is represented by the 5th percentile of each curve. All curves use the same marker styles as in Fig. 1a.

MMSE precoding, respectively. However, using only optimal power optimization remains inadequate—its curves show limited rightward extension compared to ideal cases, indicating its sensitivity to PA nonlinearity.

- *Joint Optimization:* Our proposed approach significantly enhances performance (MR: 0.3514, RZF: 0.3602, MMSE: 0.3586 bps/Hz), visualized through *Right-shifted CDF curves* approaching that of ideal PA. It remarkably outperforms the max-min power optimization, achieving improvement gains of approximately 1115 %, 276 %, and 1238 % in 95%-likely SE for MR, RZF, and MMSE precoding, respectively. These results validate the effectiveness of jointly optimizing user associations and power control in mitigating PA nonlinear effects.

Due to the dynamic nature of the bisection method—where the number of iterations required to determine the optimal variables varies—it is not feasible to evaluate complexity numerically. Therefore, we use the average runtime as a practical metric to evaluate the computational cost. All simulations were performed on a desktop computer equipped with an Intel i7-4790 processor and 32GB of memory. The average time costs observed were approximately 17.07, 7.6, and 7.1 seconds for JUP, max-min, and JUP-Lo, respectively, as shown in Fig.2. While maintaining lower complexity, the simplified approach still outperforms conventional baselines. It achieves consistent 95%-likely performance across all precoding schemes (MR: 0.0531, RZF: 0.0548, MMSE: 0.0567 bps/Hz). These results represent a  $2.1\times$  improvement over max-min power control (0.0268 bps/Hz) and a  $178\times$  enhancement compared to UC (0.0003 bps/Hz) under MMSE precoding.

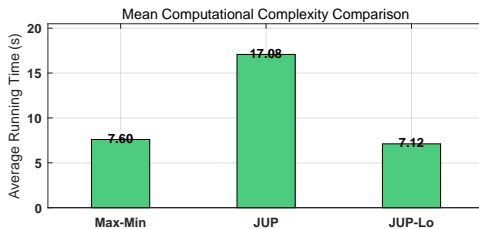


Fig. 2. Comparison of computational complexity.

## VII. CONCLUSION

This letter has addressed the critical challenge of PA nonlinearity in cell-free massive MIMO downlink systems. We proposed a unified analytical framework that models PA-induced distortion across arbitrary linear precoding schemes. Then, a joint optimization approach of user association and power control was developed to suppress PA nonlinearity. This joint approach, as well as its low-complexity variant, remarkably outperforms conventional hardware-agnostic baselines in terms of 95%-likely performance, achieving the aim of offering uniformly high-quality service. The proposed approaches provide a foundational framework for building nonlinear PA-resilient CF architectures in next-generation networks.

## REFERENCES

- [1] W. Jiang and F.-L. Luo, "Cellular and cell-free massive MIMO techniques in 6G," in *6G Key Technologies: A Comprehensive Guide*. New York, USA: John Wiley&Sons and IEEE Press, 2023, ch. 9, pp. 417 – 474.
- [2] Z. Mokhtari and R. Dinis, "Sum-rate of cell-free massive MIMO systems with power amplifier non-linearity," *IEEE Access*, vol. 9, p. 141927–141937, Oct. 2021.
- [3] M. M. Jadidi *et al.*, "Performance analysis and power allocation for uplink cell-free massive MIMO system with nonlinear power amplifier," *IEEE Trans. Commun.*, vol. 72, no. 9, pp. 5473–5485, Sep. 2024.
- [4] A. M. Khoueini *et al.*, "Performance analysis and power allocation for downlink cell-free massive MIMO system with nonlinear power amplifier," *IEEE Trans. Green Commun. Netw.*, Apr. 2025, Early Access.
- [5] S. Buzzi *et al.*, "User-centric 5G cellular networks: Resource allocation and comparison with the cell-free massive MIMO approach," *IEEE Trans. Wireless Commun.*, vol. 19, no. 2, pp. 1250–1264, Feb. 2020.
- [6] E. Nayeibi *et al.*, "Precoding and power optimization in cell-free massive MIMO systems," *IEEE Trans. Wireless Commun.*, vol. 16, no. 7, pp. 4445–4459, Jul. 2017.
- [7] E. Björnson and L. Sanguinetti, "Making cell-free massive MIMO competitive with MMSE processing and centralized implementation," *IEEE Trans. Wireless Commun.*, vol. 19, no. 1, pp. 77 – 90, Jan. 2020.
- [8] H. Q. Ngo *et al.*, "Cell-free massive MIMO versus small cells," *IEEE Trans. Wireless Commun.*, vol. 16, no. 3, pp. 1834–1850, Mar. 2017.
- [9] E. Björnson, J. Hoydis, and L. Sanguinetti, "Massive MIMO networks: Spectral, energy, and hardware efficiency," *Foundations and Trends in Signal Processing*, vol. 11, no. 3–4, pp. 154–655, 2017.
- [10] M. Grant and S. Boyd, *CVX: Matlab Software for Disciplined Convex Programming*, CVX Research, Inc., 2014.
- [11] Gurobi Optimization, LLC, *Gurobi Optimizer Reference Manual*, 2024. [Online]. Available: <https://www.gurobi.com>